arXiv:1207.6039v1 [quant-ph] 25 Jul 2012

High cooperativity in coupled microwave resonator ferrimagnetic insulator hybrids

Hans Huebl,[1, *] Christoph Zollitsch,[1] Johannes Lotze,[1] Fredrik Hocke,[1] Moritz Greifenstein,[1] Achim Marx,[1] Rudolf Gross,[1, 2] and Sebastian T. B. Goennenwein[1]
[1] *Walther-Meißner-Institut, Bayerische Akademie der Wissenschaften, Garching, Germany*
[2] *Physik-Department, Technische Universität München, Garching, Germany*

(Dated: July 26, 2012)

We report the observation of strong coupling between the exchange-coupled spins in gallium-doped yttrium iron garnet and a superconducting coplanar microwave resonator made from Nb. The measured coupling rate of 450 MHz is proportional to the square-root of the number of exchange-coupled spins and well exceeds the loss rate of 50 MHz of the spin system. This demonstrates that exchange coupled systems are suitable for cavity quantum electrodynamics experiments, while allowing high integration densities due to their extraordinary high spin densities. Our results furthermore show, that experiments with multiple exchange-coupled spin systems interacting via a single resonator are within reach.

PACS numbers: 85.25.-j, 85.70.Ge, 42.50.Pq, 76.30.+g
Keywords: ferromagnetic resonance, ferrimagnetic resonance, strong coupling, cavity quantum electrodynamics, YIG, yttrium iron garnet, low temperatures, microwave spectroscopy

The study of the interaction of matter and light on the quantum level is at the core of solid state quantum information systems. Strong [1, 2] and ultra-strong coupling [3, 4] has been achieved, allowing for the coherent transfer of quantum information. For the practical implementations of quantum information systems, the use of hybrid systems has been suggested. In such hybrids, natural microscopic systems (atoms, molecules, electron spins, and nuclear spins) are coupled with artificial meso-scale structures such as superconducting quantum circuits by means of microwave photons. Whereas the former have long coherence times due to sufficient decoupling from environmental noise, the latter allow for fast qubit gates due to strong coupling to electromagnetic fields [5]. While a large variety of hybrid systems has been proposed [6–8], ensembles of electron spins as quantum memories [9, 10] seem most promising and their coupling to superconducting resonators [11–17] and flux qubits [18] has been studied recently. Although the coupling strength g of an individual spin to an electromagnetic mode of a superconducting microwave resonator is small (typically in the order of 10 Hz), the coupling of an ensemble of N spins is enhanced by a factor of $\sqrt{N}$ [19, 20]. In this way, strong coupling $g_{\text{eff}} = g\sqrt{N} \gg \kappa, \gamma$ can be realized, where κ and γ are the loss rates of the resonator and spin system, respectively. With loss rates in the order of MHz, typically 10^{12} spins are needed to reach the strong coupling regime. Therefore, the spin system has to fill a major part of the small mode volume of a superconducting resonator. Until today, mostly paramagnetic systems consisting of ensembles of noninteracting spins have been studied. The coherent coupling of microwave resonators to ferromagnetic systems with strongly exchange coupled spins remains to be explored. Soykal and Flatté [21, 22] theoretically discussed the strong coupling of photonic and magnetic modes in exchange locked ferromagnetic systems. One particular advantage of, ferromagnetic systems is their higher spin density. Therefore, for the same number N of spins, their volume can be reduced considerable compared to paramagnetic systems. This should allow one to couple multiple spin ensembles to the same microwave resonator.

In this letter, we investigate the coupling between the electromagnetic modes of a superconducting coplanar waveguide microwave resonator and the magnetic modes of the exchange-locked ferrimagnet yttrium iron garnet ($Y_3Fe_5O_{12}$ or YIG) doped with gallium (YIG:Ga). We measure a coupling rate of $g_{\text{eff}}/2\pi = 450\,\text{MHz}$ exceeding both the spin relaxation rate $\gamma/2\pi = 50\,\text{MHz}$ and the resonator decay rate $\kappa/2\pi = 3\,\text{MHz}$. That is, we observe strong coupling. The measured effective coupling strength follows $g_{\text{eff}} = g\sqrt{N}$, where the number of spins interacting with the resonator is estimated from the sample geometry. Furthermore, the measured relaxation rate of the spin system is fully consistent with the natural linewidth of YIG:Ga obtained from ferromagnetic resonance (FMR) measurements. We note that YIG is one of the prime candidates for studying strong coupling between exchange locked spins and the electromagnetic modes of a microwave resonator. It is known to have excellent microwave properties, in particular a very small FMR linewidth of $\approx 10\,\mu\text{T}$ at 4 K and $\omega/2\pi = 9.3\,\text{GHz}$ [23]. This narrow linewidth corresponds to a T_2 time in the order of microseconds [24]. Since high quality YIG thin films can be prepared on various substrates (gadolinium gallium garnet [25, 26], Si and GaAs [27]) and doped with rare earth elements in order to adjust the FMR linewidth in a controlled way. YIG appears like an ideal material for ferromagnet based quantum hybrids.

As pointed out by Soykal and Flatté [21, 22], in a macrospin approximation the Hamiltonian for the

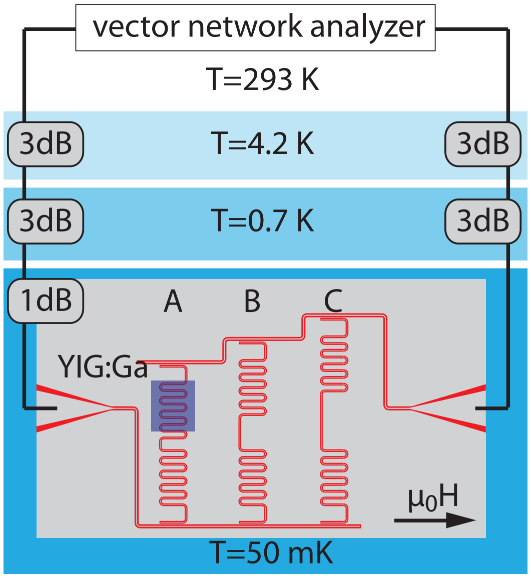

FIG. 1. Schematic of the experimental setup. The (purple) gallium doped YIG sample is cemented ontop of one of the niobium microwave resonators which are arranged to allow for multiplexing. Experiments are performed at millikelvin temperatures in transmission by vector network analysis in a superconducting solenoid magnet.

ferromagnet-resonator system can be expressed as

$$\mathcal{H} = \hbar\omega_r a^\dagger a + \frac{g_s \mu_\mathrm{B} B_z}{\hbar} S_z + \hbar g (a S_+ + a^\dagger S_-). \qquad (1)$$

Here, $a^\dagger$ and a are the photon creation/annihilation operators, ω_r the resonator frequency, g_s is the electron g-factor, μ_B the Bohr magneton, and B_z the applied magnetic field establishing the resonance condition $\hbar\omega_\mathrm{FMR} = g_s \mu_\mathrm{B} B_z/\hbar$ between the microwave field and the energy level splitting of the ferromagnet. The macrospin operator $\mathbf{S} = (S_+ \hat{\mathbf{e}}_- - S_- \hat{\mathbf{e}}_+)/\sqrt{2} + S_z \hat{\mathbf{z}}$ with $\hat{\mathbf{e}}_\pm = \mp(\hat{\mathbf{x}} \pm \imath\hat{\mathbf{y}})/\sqrt{2}$ is expressed in terms of the spin lowering and raising operators

$$S_\pm \left| \frac{N}{2}, m \right\rangle = \sqrt{\left(\frac{N}{2} \mp m\right)\left(\frac{N}{2} \pm m + 1\right)} \left| \frac{N}{2}, m \pm 1 \right\rangle . \qquad (2)$$

Here, $|\ell, m\rangle$ are the eigenstates of the macrospin and we have assumed that the macrospin state is fixed at its maximal value $\ell = N/2$. In the Dicke model [28] of N independent paramagnetic spins this would correspond to a fully excited spin system with no photons in the cavity. In contrast to the Dicke model, for our macrospin model states with $\ell < N/2$ are not accessible. Due to strong exchange coupling, states with $\ell < N/2$ are separated in energy and require the excitation of magnons. We note that the coupling between the photonic and magnetic system is a magnetic dipole transition and that the Hamiltonian (1) conserves the total excitation number $Z = n + m$, where n is the photon number in the cavity and $|m| \leq \ell = N/2$ the magnetic quantum number. Assuming that $\mathbf{S}$ is antiparallel to B_z and $n = 0$ initially, we have $Z = N/2$ and, hence, can index the basis states $|n, m\rangle$ of the resonator-spin systems either by the photon number n ($|n, \frac{N}{2} - n\rangle$) or the magnetic quantum number m ($|\frac{N}{2} - m, m\rangle$). Evidently, these basis states are similar to those of the Dicke model [28] for a paramagnetic ensemble of N noninteracting spins coupled to a resonator, with $\ell = N/2$ taking the role of the cooperation number. Note that the coupling between the ferromagnet and the resonator modes changes over a wide range when moving through all possible states $|n, \frac{N}{2} - n\rangle$ with an equilibrium point at $n_0 = (2N-1)/3$, where the ferromagnet-resonator systems shows superradiance [28].

Due to the analogy with the Dicke model, we expect that the coupling strength of the ferromagnet-resonator system is given by the effective coupling strength $g_\mathrm{eff} = g\sqrt{N}$ of a paramagnet-resonator system, where $g = \frac{g_s \mu_B}{2\hbar} B_{1,0}$ is the coupling rate of an individual spin with the magnetic quantum number $m = 1/2$ to the resonator [28]. It is determined by the magnetic component of the rf vacuum field $B_{1,0} = \sqrt{\mu_0 \hbar \omega_\mathrm{c}/2V_\mathrm{m}}$ which depends on the resonance frequency of the microwave resonator ω_c and the mode volume V_m of the resonator [29]. Hence, for a given resonance frequency, $g_\mathrm{eff} = \frac{g_s \mu_B}{2\hbar}\sqrt{\mu_0 \rho \hbar \omega_\mathrm{r} V/2V_\mathrm{m}}$ depends only on the spin density $\rho = N/V$ and the filling factor V/V_m, where V denotes the volume of the overlap between the spin system and the resonator field mode. Non-interacting spin ensembles like paramagnetic centers in semiconductors or insulators typically have a spin density ρ in the order of $10^{15} \leq \rho \leq 10^{18}\,\mathrm{cm}^{-3}$ [11, 12, 14]. In combination with resonator frequencies in the 5 GHz range, this results in coupling rates in the order of 10 MHz assuming $V/V_\mathrm{m} \simeq 1$. In contrast, exchange coupled systems naturally have a spin density in the order of one per atom (e.g. Fe, Ni, Co) or in the case of YIG 40 per unit cell (unit cell volume: $a^3 = 1.8956\,\mathrm{nm}^3$), corresponding to a spin density of $2\times10^{22}\,\mathrm{cm}^{-3}$ [30]. Due to the increase of at least four orders of magnitude in the spin density we expect in exchange coupled systems a two orders larger coupling strength as compared to non-interacting spins using similar microwave resonators. In other words, in exchange coupled systems the sample volume of the spin system can be reduced by a factor of 10^4 while keeping the coupling rate constant, thereby allowing for a much higher integration density.

In our experiments, we study the coupling between the exchange locked system YIG:Ga and a superconducting Nb resonator. The resonator structure is patterned into a 100 nm thick Nb film deposited onto an intrinsic silicon substrate using optical lithography and reactive ion etching [29]. Figure 1 shows the layout of the microwave circuitry consisting of an input line, three resonators with resonance frequencies of $f_A = 5.90\,\mathrm{GHz}$, $f_B = 5.53\,\mathrm{GHz}$, and $f_C = 5.30\,\mathrm{GHz}$, and an output line. This configuration allows to compare loaded and unloaded microwave

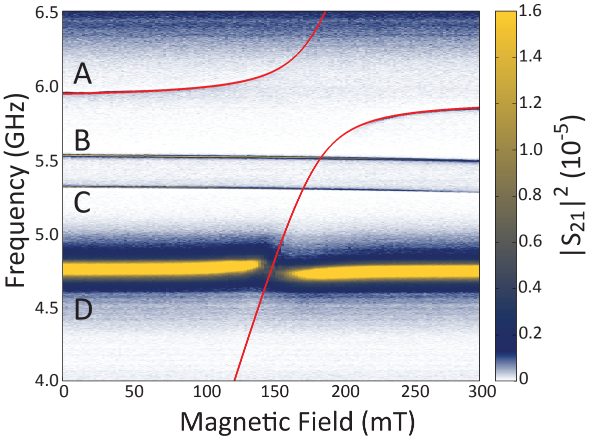

FIG. 2. Transmission spectrum of the YIG-microwave resonator hybrid taken at $T = 50\,\mathrm{mK}$ as a function of the applied magnetic field B_z. The coplanar waveguide resonators (A-C) show a slightly decreasing resonance frequency with increasing in-plane magnetic field. Additionally, resonator A shows a pronounced avoided crossing at $B_{z,\mathrm{r}} = 170\,\mathrm{mT}$, where the resonance condition $\hbar\omega_\mathrm{r} = g_s\mu_\mathrm{B}B_{z,\mathrm{r}}/\hbar$ between the resonator and the energy level splitting of the ferromagnet is satisfied. The red line shows a fit according to eq.(3).

resonators on the same chip. A $2 \times 0.5 \times 0.7\mathrm{mm}^3$ sized (length × width × thickness) commercial YIG:Ga crystal is cemented onto resonator A with the highest microwave frequency $f_A = 5.90\,\mathrm{GHz}$. The number of spins interacting with the resonator is estimated from the overlap of the YIG:Ga crystal with the meandering coplanar waveguide with a center conductor width of 6 µm and a gap of 12 µm. With the overlap length of 2.5 mm and assuming that the vertical extension of the microwave field into the YIG crystal is about 30 µm, the total number of spins coupled to the resonator is estimated to $N \approx 4.5 \times 10^{16}$. To preserve the superconducting state of the microwave resonators, the surface of the chip is carefully aligned in parallel to the applied magnetic field B_z generated by a superconducting solenoid. The microwave transmission experiments are performed at the base temperature of a dilution refrigerator of 50 mK using a commercial vector network analyzer. To thermalize the microwave input and output lines, attenuators are used at the 4 K, the still and the mixing chamber stages.

Figure 2 shows the microwave transmission $|S_{21}|^2$ as a function of frequency and applied magnetic field. Hereby, S_{21} is the complex scattering parameter. In the spectrum at $B_z = 0$, four transmission peaks are visible corresponding to the resonance frequencies of the coplanar microwave resonators A, B, and C. The broad feature labeled D stems from a parasitic mode of the metallic microwave box in which the sample is mounted. As expected, the resonators B and C show only a weak magnetic field dependence, because they are not interacting with the YIG:Ga crystal due to the absence of physical overlap (cf. Figs. 1 and 2). On the contrary, resonator A and the box mode D couple to the magnetic system. While mode D allows us to probe the ferromagnetic resonance independently of the strongly coupled mode (A) and to determine the resonance condition, resonator A shows a distinct anticrossing at $B_{z,\mathrm{r}} = 170\,\mathrm{mT}$ where the resonance condition $\hbar\omega_\mathrm{r} = g_s\mu_\mathrm{B}B_{z,\mathrm{r}}/\hbar$ between the resonator frequency and the energy level splitting of the ferromagnet is satisfied.

To derive the effective coupling rate g_eff from the measured data, we model the ferrimagnet-resonator interaction according to two-level atom theory. Within this approach, the dispersion of the resonance frequency is given by [31]

$$\omega = \omega_\mathrm{r} + \frac{\Delta}{2} \pm \frac{1}{2}\sqrt{\Delta^2 + 4g_\mathrm{eff}^2}\,. \tag{3}$$

Here, $\Delta = \omega_\mathrm{r} - \omega_\mathrm{FMR} = g_s\mu_\mathrm{B}(B_{z,\mathrm{r}} - B_\mathrm{FMR})/\hbar$ is the field dependent detuning between the resonator frequency ω_r and the field dependent FMR frequency ω_FMR. The experimental data agree very well with this model prediction. Fitting the data yields $g_\mathrm{eff} = 450\,\mathrm{MHz}$ and $B_\mathrm{FMR} = 170\,\mathrm{mT}$, using the g-factor of the ferrimagnetic resonance $g_s = 2.17$. For the geometry of our resonator we estimate $g/2\pi \simeq 5\,\mathrm{Hz}$ and $N \simeq 4 \times 10^{16}$. With these numbers we expect $g_\mathrm{eff}/2\pi = (g/2\pi)\sqrt{N} \simeq 1\,\mathrm{GHz}$ corroborating our experimental result within a factor of two. We point out that no gap has been assumed between the microwave resonator and the YIG:Ga sample in our estimate of g and N. This most likely is not the case in the actual sample configuration due to imperfections in the sample mounting process. Here, an additional gap between the superconducting niobium layer and the YIG:Ga would result in a decrease in N. We finally note that the frequency dispersion of the ferromagnetic mode compares well with values from Ref. [32], whereas the g-factor of 2.17 is about 10 % larger than $g_s = 2.0$ reported for room temperature YIG [32]. This is attributed to an imperfect calibration of the magnetic field produced by the superconducting solenoid.

To get information on the relaxation rate γ of the spin system we analyze the evolution of the linewidth of the resonator mode A as a function of the magnetic field B_z by fitting a Lorentzian lineshape in the frequency domain for every measured magnetic field magnitude [17]. Figure 3(a) shows the resonance frequency obtained from such a fit as red crosses superimposed on the color-coded dataset. In Fig. 3(b) the corresponding (FWHM) linewidth (red crosses) is shown. At low magnetic fields, the resonator mode A is essentially decoupled from the spin system. In this regime the measured linewidth is given by the resonator loss rate κ. Closer to the ferromagnetic resonance, the linewidth of the system is given by the combined relaxation rate of the spin system and the microwave resonator leading to an increase in the observed linewidth.

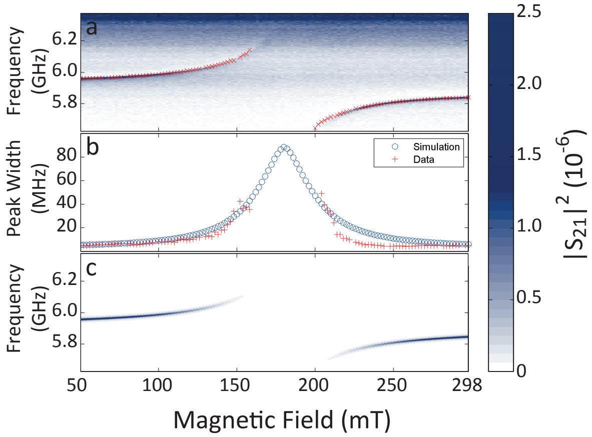

FIG. 3. Analysis of the resonance frequency and linewidth as a function of the magnetic field B_z. Panel (a) shows the resonator transmission $|S_{21}|^2$ (same data as Fig. 2) as a function of frequency and applied magnetic field. The red crosses mark the resonance frequency determined by fitting a Lorentzian lineshape to the data at constant B_z. The red crosses in panel (b) show the extracted FWHM linewidths. In addition, the blue circles show the linewidths obtained from the numerical simulation of the transmission spectra plotted in panel (c). The simulation is based on the input-output formalism resulting in eq.(4) [11, 17, 20, 33].

We now analyze the measured data in more detail to quantify the coupling and loss rates in our system. Here, we use a standard input-output formalism [11, 17, 20, 33]. Within this framework the transmission of microwaves from the input to the output port of the microwave resonator is given by

$$S_{21} = \frac{\kappa_{\mathrm{c}}}{\imath(\omega - \omega_{\mathrm{r}}) - (\kappa_{\mathrm{c}} + \kappa_{\mathrm{i}}) + \frac{|g_{\mathrm{eff}}|^2}{\imath(\omega - \omega_{\mathrm{FMR}}) - \gamma_{\mathrm{S}}/2}} \,. \qquad (4)$$

Here, $\omega/2\pi$ is the frequency of the microwave probe tone, κ_{c} is the external coupling rate between the microwave resonator and the feed line, and κ_{i} summarizes the intrinsic loss rate of the microwave resonator. In our case we have $\kappa_{\mathrm{i}} \ll \kappa_{\mathrm{c}}$, resulting in a total microwave resonator relaxation rate $\kappa \simeq \kappa_{\mathrm{c}}$. Fig. 3(c) shows the calculated transmission using $g_{\mathrm{eff}}/2\pi = 450\,\mathrm{MHz}$, $\gamma/2\pi = 50\,\mathrm{MHz}$, and $\kappa/2\pi = 3\,\mathrm{MHz}$. Evidently all features of the experimental data of Fig. 3(a) are nicely reproduced. In particular, Fig. 3(c) clearly shows that for the large cavity decay rate $\kappa/2\pi = 3\,\mathrm{MHz}$ the two transmission peaks expected at $B_{\mathrm{res}} = 170\,\mathrm{mT}$ cannot be resolved due to the limited signal to noise ratio in the experimental data. Moreover, we can analyze the simulation data shown in Fig. 3(c) in the same way as the experimental data in Fig. 3(a) to derive the field dependence of the linewidth. The result is shown by the blue circles in Fig. 3(b), where in contrast to the experimental data, the modeled data is noise-free allowing to predict the linewidth for all magnetic field values. The good agreement between experimental and simulation data again demonstrates that the parameters chosen in the simulation well reproduce the experimental situation. In summary, our analysis shows that $g_{\mathrm{eff}} \gg \kappa, \gamma$ with a cooperativity $C = g_{\mathrm{eff}}^2/\kappa\gamma \simeq 1350$. That is, the strong coupling regime has been reached for the ferrimagnet-resonator system.

Finally, we compare the experimentally determined relaxation rate γ with measurements of the temperature dependence of the FMR linewidth performed at 9.43 GHz. Rachford *et al.* [34] report linewidth values for lightly Ga doped YIG that decrease from 1 mT at liquid helium temperatures to 0.1 mT at room temperature, corresponding to 28 MHz and 2.8 MHz, respectively. Our sample has a higher Ga-doping concentration [35], which is known to result in an increase of the linewidth. This is consistent with the relaxation rate of $\gamma/2\pi = 50\,\mathrm{MHz}$ observed in our experiments at millikelvin temperatures. Although, we would like to stress that little is known about the evolution of damping in YIG for $T \leq 2\,\mathrm{K}$, according to Sparks and Kittel [36] the limiting relaxation mechanism is spin-lattice coupling, which is expected to be well below 1 MHz for YIG.

In conclusion, we experimentally observed strong coupling between a superconducting microwave resonator and a gallium doped yttrium iron garnet ferrimagnet. The effective coupling rate of 450 MHz reaches 13% of the resonator frequency ω_{r} and by far exceeds the relaxation rate $\gamma/2\pi = 50\,\mathrm{MHz}$ of the spin system. Therefore, exchange coupled spin systems indeed can be used for cavity quantum electrodynamics. Furthermore, the large coupling rates achievable in exchange coupled systems allow to place more than a single magnetic system in the microwave resonator. This should allow to study e.g. the exchange of magnetic excitations via a cavity bus similar to the approaches pursued in the field of cavity QED [5].

We gratefully acknowledge technical support by Matthias Opel. This work is supported by the German Research Foundation through SFB 631 and the German Excellence Initiative via the “Nanosystems Initiative Munich” (NIM).

---

[*] corresponding author huebl@wmi.badw.de

[1] A. Wallraff, D. I. Schuster, A. Blais, L. Frunzio, R.-S. Huang, J. Majer, S. Kumar, S. M. Girvin, and R. J. Schoelkopf, Nature **431**, 162 (2004).
[2] R. J. Schoelkopf and S. M. Girvin, Nature **451**, 664 (2008).
[3] T. Niemczyk, F. Deppe, H. Huebl, E. P. Menzel, F. Hocke, M. J. Schwarz, J. J. Garcia-Ripoll, D. Zueco, T. Hümmer, E. Solano, A. Marx, and R. Gross, Nat. Phys. **6**, 772 (2010).
[4] J. P. Reithmaier, G. Sęk, A. Löffler, C. Hofmann, S. Kuhn, S. Reitzenstein, L. V. Keldysh, V. D. Kulakovskii, T. L. Reinecke, and A. Forchel, Nature **432**, 197 (2004).
[5] L. DiCarlo, J. M. Chow, J. M. Gambetta, L. S. Bishop,

B. R. Johnson, D. I. Schuster, J. Majer, A. Blais, L. Frunzio, S. M. Girvin, and R. J. Schoelkopf, Nature **460**, 240 (2009).

[6] A. AndrÃ©, D. DeMille, J. M. Doyle, M. D. Lukin, S. E. Maxwell, P. Rabl, R. J. Schoelkopf, and P. Zoller, Nat. Phys. **2**, 636 (2006).

[7] J. Verdú, H. Zoubi, C. Koller, J. Majer, H. Ritsch, and J. Schmiedmayer, Phys. Rev. Lett. **103**, 043603 (2009).

[8] M. Wallquist, K. Hammerer, P. Rabl, M. Lukin, and P. Zoller, Phys. Scr. T **137** (2009).

[9] J. Wesenberg, A. Ardavan, G. Briggs, J. Morton, R. Schoelkopf, D. Schuster, and K. Molmer, Phys. Rev. Lett. **103** (2009).

[10] A. Imamoglu, Phys. Rev. Lett. **102**, 083602 (2009).

[11] D. I. Schuster, A. P. Sears, E. Ginossar, L. DiCarlo, L. Frunzio, J. J. L. Morton, H. Wu, G. A. D. Briggs, B. B. Buckley, D. D. Awschalom, and R. J. Schoelkopf, Phys. Rev. Lett. **105**, 140501 (2010).

[12] Y. Kubo, F. R. Ong, P. Bertet, D. Vion, V. Jacques, D. Zheng, A. Dreau, J. F. Roch, A. Auffeves, F. Jelezko, J. Wrachtrup, M. F. Barthe, P. Bergonzo, and D. Esteve, Phys. Rev. Lett. **105**, 140502 (2010).

[13] Y. Kubo, C. Grezes, A. Dewes, T. Umeda, J. Isoya, H. Sumiya, N. Morishita, H. Abe, S. Onoda, T. Ohshima, V. Jacques, A. Dréau, J.-F. Roch, I. Diniz, A. Auffeves, D. Vion, D. Esteve, and P. Bertet, Phys. Rev. Lett. **107**, 220501 (2011).

[14] R. Amsüss, C. Koller, T. Nöbauer, S. Putz, S. Rotter, K. Sandner, S. Schneider, M. Schramböck, G. Steinhauser, H. Ritsch, J. Schmiedmayer, and J. Majer, Phys. Rev. Lett. **107**, 060502 (2011).

[15] I. Chiorescu, N. Groll, S. Bertaina, T. Mori, and S. Miyashita, Phys. Rev. B **82**, 024413 (2010).

[16] P. Bushev, A. K. Feofanov, H. Rotzinger, I. Protopopov, J. H. Cole, C. M. Wilson, G. Fischer, A. Lukashenko, and A. V. Ustinov, Phys. Rev. B **84**, 060501 (2011).

[17] E. Abe, H. Wu, A. Ardavan, and J. J. L. Morton, Appl. Phys. Lett. **98**, 251108 (2011).

[18] X. Zhu, S. Saito, A. Kemp, K. Kakuyanagi, S. Karimoto, H. Nakano, W. J. Munro, Y. Tokura, M. S. Everitt, K. Nemoto, M. Kasu, N. Mizuochi, and K. Semba, Nature **478**, 221 (2011).

[19] M. G. Raizen, R. J. Thompson, R. J. Brecha, H. J. Kimble, and H. J. Carmichael, Phys. Rev. Lett. **63**, 240 (1989).

[20] D. F. Walls and G. J. Milburn, *Quantum Optics*, 1st ed. (Springer, Berlin, 1994).

[21] O. O. Soykal and M. E. Flatté, Phys. Rev. B **82**, 104413 (2010).

[22] O. O. Soykal and M. E. Flatté, Phys. Rev. Lett. **104**, 077202 (2010).

[23] E. G. Spencer, R. C. LeCraw, and A. M. Clogston, Phys. Rev. Lett. **3**, 32 (1959).

[24] D. E. Kaplan, Phys. Rev. Lett. **14**, 254 (1965).

[25] S. A. Manuilov, R. Fors, S. I. Khartsev, and A. M. Grishin, J. Appl. Phys. **105**, 033917 (2009).

[26] S. A. Manuilov and A. M. Grishin, J. Appl. Phys. **108**, 013902 (2010).

[27] M. Levy, R. M. Osgood, A. Kumar, and H. Bakhru, Appl. Phys. Lett. **71**, 2617 (1997).

[28] R. H. Dicke, Phys. Rev. **93**, 99 (1954).

[29] T. Niemczyk, F. Deppe, M. Mariantoni, E. P. Menzel, E. Hoffmann, G. Wild, L. Eggenstein, A. Marx, and R. Gross, Supercond. Sci. Tech. **22**, 034009 (2009).

[30] M. Gilleo and S. Geller, Phys. Rev. **110**, 73 (1958).

[31] S. Haroche and J. M. Raimond, *Exploring the Quantum: Atoms, Cavities and Photons* (Oxford University Press, Oxford, 2006).

[32] S. A. Manuilov, S. I. Khartsev, and A. M. Grishin, J. Appl. Phys. **106**, 123917 (2009).

[33] A. A. Clerk, S. M. Girvin, F. Marquardt, and R. J. Schoelkopf, Rev. Mod. Phys. **82**, 1155 (2010).

[34] F. J. Rachford, M. Levy, R. M. Osgood, A. Kumar, and H. Bakhru, J. Appl. Phys. **87**, 6253 (2000).

[35] *YIG:Ga Datasheet - www.ferrisphere.com.*

[36] M. Sparks and C. Kittel, Phys. Rev. Lett. **4**, 232 (1960).